

## Study on some factors affecting Ground-Pile-Tunnelling interaction

Mona M. Eid, Ali A. A. Ahmed, Ashraf M. Hefny, and Ahmed N. EL-Attar

Department of Geotechnical Engineering, Faculty of Engineering, Ain Shams University, Cairo, Egypt  
Ahmed\_civil\_hti@yahoo.com

**Abstract:** Tunnelling in urban area may inevitably affect the stability of overlying or nearby piling systems. Many interrelated factors are arising in analysing such complicated problems related to the employed tunnelling technology, the boundary conditions of the ground formations, and the configuration of the tunnel route to the piling system. In the present study, a parametric study is conducted using a 3D finite element code to investigate some factors affecting the tunnelling-soil-piles interaction. The soil convergence around the tunnel opening is modelled using a non-associated Mohr-Coulomb failure criterion. The configuration of piles tip relative to tunnel centreline and the offset distance of pile caps to tunnel centreline are evaluated. In addition, the ground continuum boundary conditions and its strength characteristics, the grouting strength behaviour from soft to hard conditions, and the shield and lining elastic parameters are idealized in the details of global ground-tunnelling-piling interaction idealization. The induced forces and deformations in the employed piling system due tunnelling are evaluated in association to the tunnel configuration. The displacement and induced force fields around the tunnel opening are used to specify both zones of high displacements and distressing zones around the tunnel opening.

[Mona M. Eid, Ali A. A. Ahmed, Ashraf M. Hefny, and Ahmed N. EL-Attar. **Study on some factors affecting Ground-Pile-Tunnelling interaction.** *J Am Sci* 2015;11(6):263-274]. (ISSN: 1545-1003). <http://www.jofamericanscience.org>. 31

**Keywords:** Tunnelling, excavation, nearby piles, 3-D finite element, foundation.

### 1. Introduction

Scarcity of land and rapid increasing population has led to frequent exploitation of underground space in dense urban areas. Unfortunately, many structures exist long before the tunnels are planned. Thus, it is increasingly complex and challenging technically to build underground tunnels which almost inevitably run close to the piles supporting the existing buildings Lee et al., (1994) and Coutts and Wang, (2000).

Quite some literatures are available on the topic of the influence of new tunnels on existing pile foundation. The first published analysis of pile-tunnel interaction quoted back to 1979 (Morton and King, 1979). Since then, the number of researches carrying out such study has tremendously increased.

Early efforts to study tunnel-soil-pile interaction have focused primarily on pile end bearing response and settlement magnitudes, neglecting induced axial force and bending behaviour. However, recent numerical studies by Cheng et al. (2004), Pang et al. (2005), Yang *et al.* (2011), Yao et al., (2012), Lee, (2012), Linlong et al., (2012), Lee, 2013, Ng et al., (2013), Dias and Bezuijen (2014), and Zidan and Ramadan, (2015) have provided valuable insight and understanding into the various factors that affect the performance of piled foundations subjected to tunnelling induced ground movements.

The response of pile foundation when subjected to tunnel construction is principally a three-dimensional problem whether it is the tunnel

advancement or the pile foundation. Three dimensional analyses are essential for more accurate prediction and give more flexibility in handling complex tunnelling process and soil condition.

In this paper, a parametric study is performed to examine the influence of tunnelling on adjacent piled foundations. The influences of the following parameters are assessed: pile-tunnel distance ( $X_{pile}/D_{tun}$ ), and pile length to tunnel depth ratio ( $L_p/H$ ). Full tunnel construction process including the application of face pressure, shield advancement, over-cutting, tail void closure and installation of lining was simulated in this paper.

### 2. The Reference Case (The Calibrated Model)

The closer pile cap of Garage EL-Attaba to the tunnel route of Cairo Metro (F1) is utilized in the analysis to evaluate the effect of variable parameters on the footing behaviour due to tunnelling process, (Fig.1). The front and rear piles are located at a distance of 0.6 and 0.9m tunnel diameter respectively. The three central piles axis are parallel to the tunnel route with a deviation of 0.7 tunnel diameter. The piles are 0.6m diameter and 20m long. The pile cap is 1.12m depth. The soil formation and the material properties used in the study are shown in Table (1). The excavated tunnel diameter is 9.55m and the lining inner diameter is 8.35m with lining thickness of 0.4m. The centreline of the tunnel located at a depth of 25.98m.

Table (1): The estimated properties for soil, lining, and structure

Layers	Average thickness (m)	$\gamma$ (kN/m <sup>3</sup> )	$\phi^\circ$	C (kN/m <sup>2</sup> )	E (MN/m <sup>2</sup> )	$\nu$	$\Psi$
Made ground	6.06	17.0	27	0.0	4	0.3	0
Silty clay	3.58	19.5	$\phi_d=29^\circ$ $\phi_u=0^\circ$	$C_d=0$ $C_u=90$	$E_d=20$ $E_u=22$	$\nu_d=0.35$ $\nu_u=0.49$	0
Upper Sand	13.81	19.5	36°	0.0	40	0.3	6
Sand gravel	1.15	20.0	41°	0.0	100	0.3	11
Middle sand	1.38	19.5	38	0.0	70	0.3	8
Lower sand	Extended	19.5	38°	0.0	120	0.3	8
Pile cap	-	25	-	-	$3.45 \times 10^4$	-	
Pile	-	25	-	-	$3.45 \times 10^4$		

Note:  $\gamma$ = soil density,  $\phi$ = the internal angle of friction, C= soil cohesion, E= Elastic modulus,  $\nu$ = the poisson's ratio,  $\Psi$ = dilation angle.

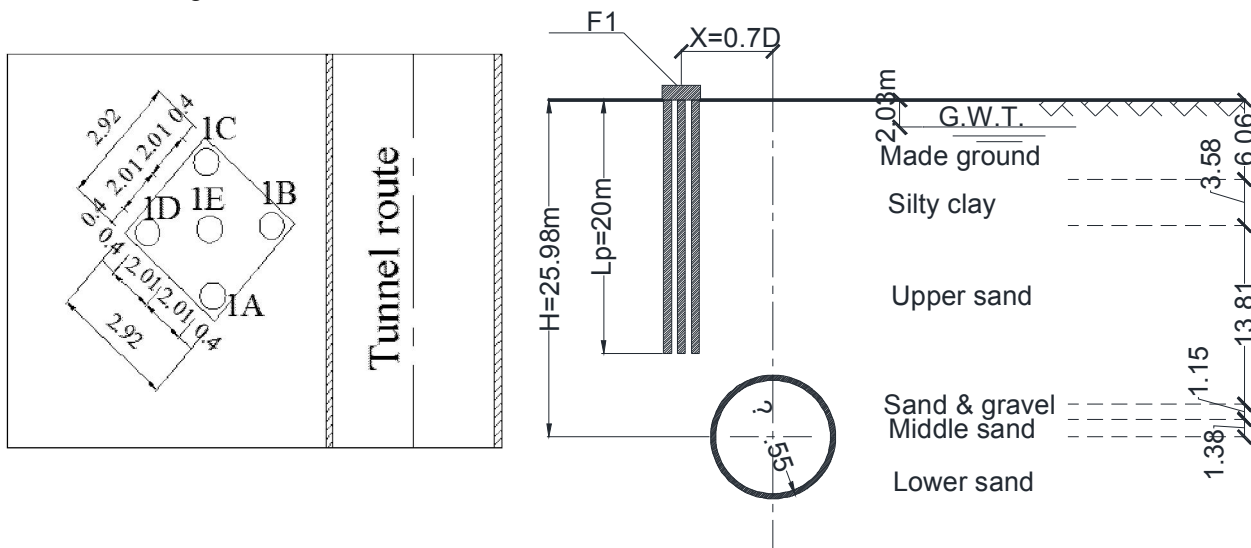


Fig.(1):Plan and cross-section views of the closer pilecap (F1) relative to the tunnel route.

### 3. Numerical modelling

The finite element mesh used to simulate the reference case is shown in Fig.(1). The finite element mesh was 120 m long, 86 m high and 128m wide. In this paper, numerical simulations were performed by means of the finite element program ABAQUS (Hibbitt, Karlsson& Sorensen Inc., 2011).

Analysis of the tunnelling–structure interaction problem is performed with two steps. The first step is concerned with the determination of initial stresses in the soil mass prior to the tunnel construction. It is performed using a finite element calculation considering the self-weight of both the soil. The initial conditions were completed with simulating the piles

and the connected pile cap. The second step deals with the numerical simulation for the construction of the tunnel in presence of the pile cap. An elastic-plastic soil model using the Mohr-coulomb failure criterion is adapted in this study. The structural properties such as lining and shield machine were modelled as linear elastic material. The shield is modelled as solid elements having ( $E= 200\text{GPa}$  and  $\nu=0.25$ ). Also, the over-cutting is modelled using solid elements having ( $E= 1000\text{ kPa}$  and  $\nu = 0.2$ ) and representing the grout properties in the liquid state, while the hardened grout is assigned to ( $E = 50\text{MPa}$  and strength of about  $0.5\text{ kPa}$  after 28 days).

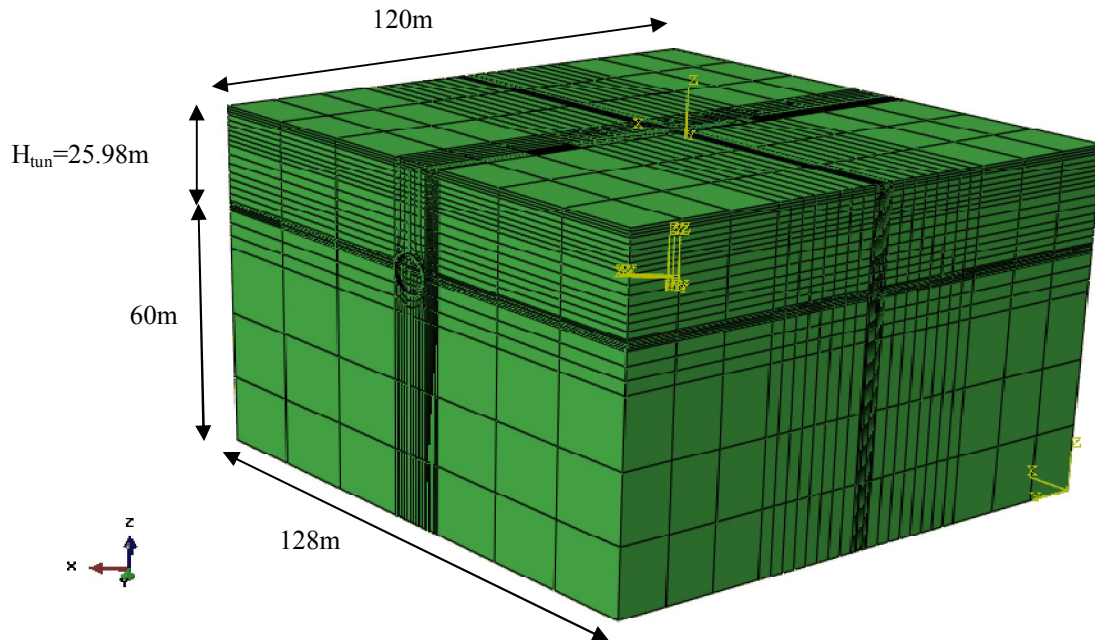


Fig.(2): Typical finite element mesh adopted.

#### 4. Parametric Studies

A set of parametric studies was carried out by varying pile length to tunnel depth ratio ( $L_p/H$ ) and the normalised tunnel-pile distance ( $X_p/D_t$ ). Fig.(3), shows the geometry and pile positions investigated,  $X_p/D_t$  of 0, 0.7, 1.0, 1.5 and 2.0 and  $L_p/H$  of 0.5, 0.6, 0.8, 1.0, and 1.4 were considered. The pile was considered stress free prior to tunnelling (i.e. without working load at the pile head).

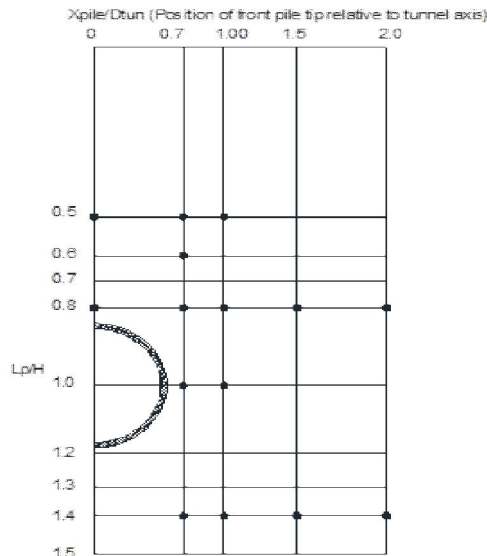


Fig.(3):Pile base position investigated in parametric studies

#### 5. Results

The results are shown in terms of vertical settlement, longitudinal displacement, lateral displacement, and axial force.

##### 5.1 Pile Settlement

Figures. (4-a,b), illustrate the rear pile vertical displacements for the different lengths due to tunnel advancement for two cases of pile caps located at a distance of 0.7, 1.0 times tunnel diameter. The green-field condition surface settlement curves for the two offset cases are presented on the figures. The figures indicate that for all pile configurations except for  $L_p/H=1.4$ , the pile settlement increases with the tunnel advancement until the TBM reaches the pile cap location, which can be attributed to face losses. A further settlement with higher rate is detected when the TBM machine passes away from the pile cap up to a distance of about 9m, which may be attributed as losses around the TBM. Then, piles settlement rates continue constant due to the hardening of the tail grout. It may be noted that the face and shield losses increase as the pile length decreases. This means that shorter piles exhibit more settlement than the longer ones depending on its bearing point relative to tunnel crown, or the zone of high displacements. In addition, the vertical displacement of piles located above the crown level with  $X_p=0.7D_t$  are more than the surface green-field condition, which indicate that the piles located in the zone bounded by  $L_p/H \leq 0.8$  and  $X_p=0.7D_t$  is characterized as critically affected by tunnelling. For  $L_p/H=1.4$ , the pile cap exhibits a minor heave increases

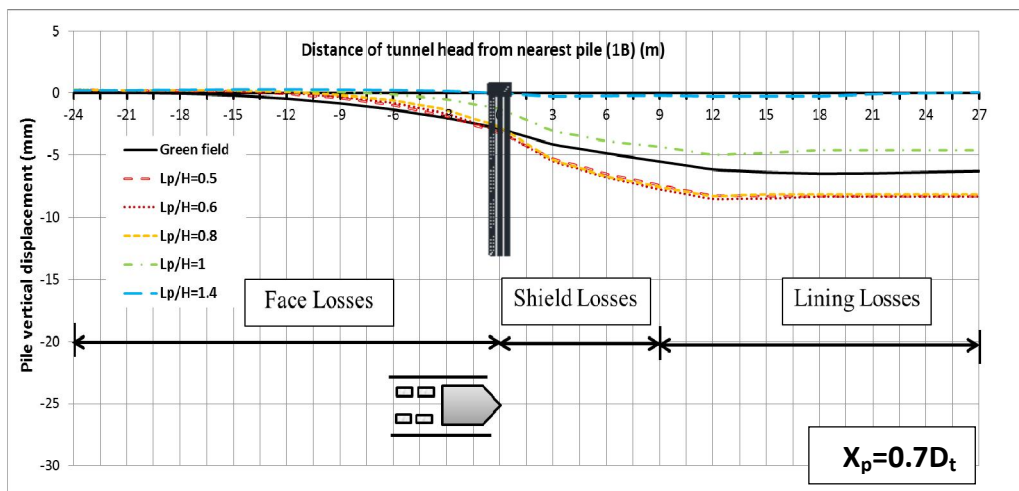
as the tunnelling proceeds until the machine reaches the pile cap location. As the tunnel advance, minor settlement can be detected. This means that longer pile settlement is not sensitive to the tunnelling operation.

### 5.2 Longitudinal Displacement

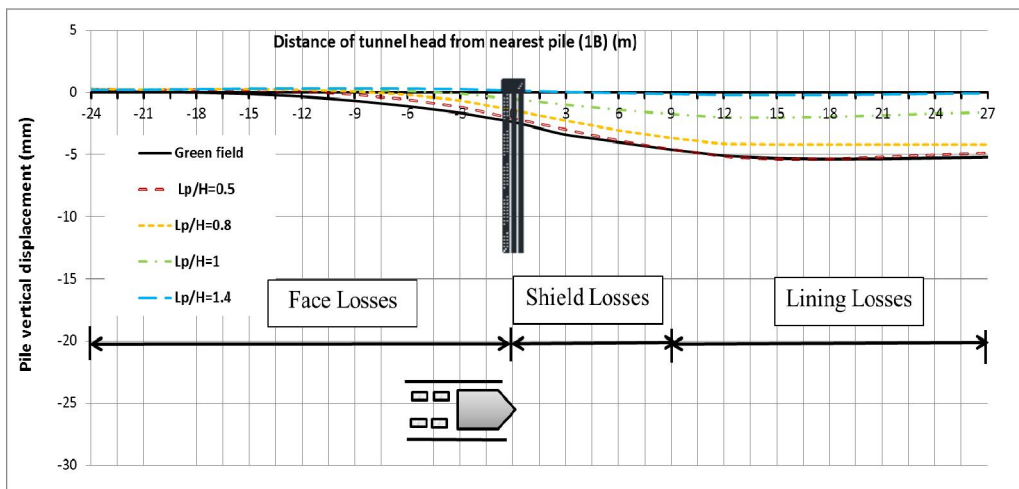
Figures (5 and 6), illustrate the horizontal longitudinal deformations of front pile due to tunnelling. The results indicate that, for all pile lengths, the longitudinal deformation of pile head starts to take place when the TBM is behind the pile cap by about 24m. The maximum longitudinal deformation occurs when the TBM reaches the location of the pile cap. Then the deformation decreases as the tunnelling proceeds and almost vanishes and the pile returns to its

initial position when the TBM is about 21m ahead of the cap. This

can be attributed to face losses of the tunnelling machine as its effect on the pile disappears as the TBM is ahead of the pile cap. For longer pile ( $L_p/H=1.0$  and  $L_p/H=1.4$ ) the lower part of the pile face the excavated tunnel moves away from the tunnel face due to the applied face pressure. It is to be mentioned that the maximum head deformation is about 2mm in the case of  $X_p=1.0D_t$  while it is about 3mm for  $X_p=0.7D_t$ . This means that as the offset increases the maximum longitudinal deformation decreases for the same pile length.



(a)



(b)

Fig. (4): The vertical displacement of front pile due to tunnel advancement for different pile length ratio and horizontal offset (a)  $X_p=0.7D_t$ , and (b)  $X_p=1.0D_t$

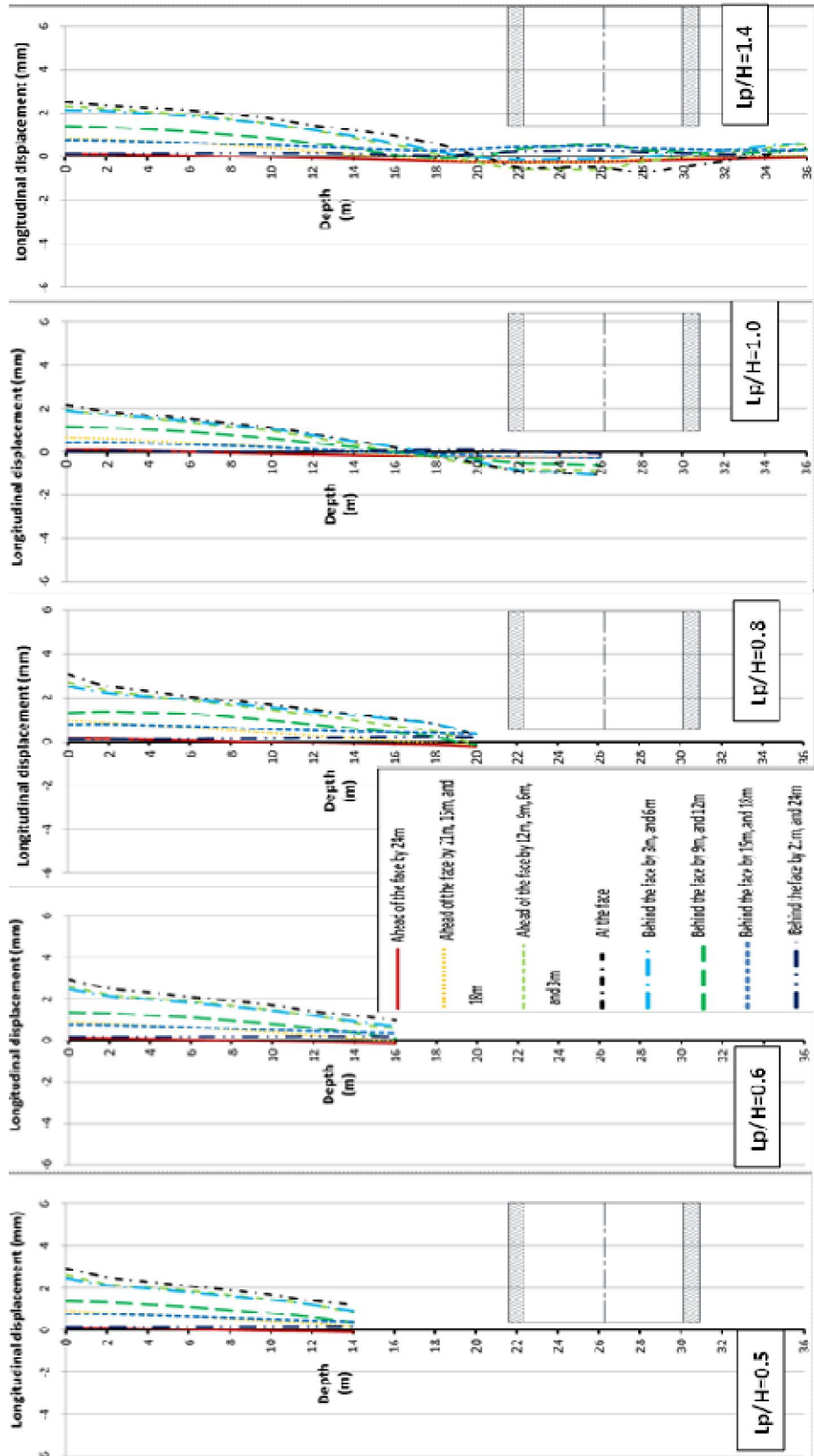


Fig.(5): Longitudinal displacement of front pile (1B) during tunnelling for different values of ( $L_p/H$ ) and at constant offset ( $X_p=0.7D_1$ ).



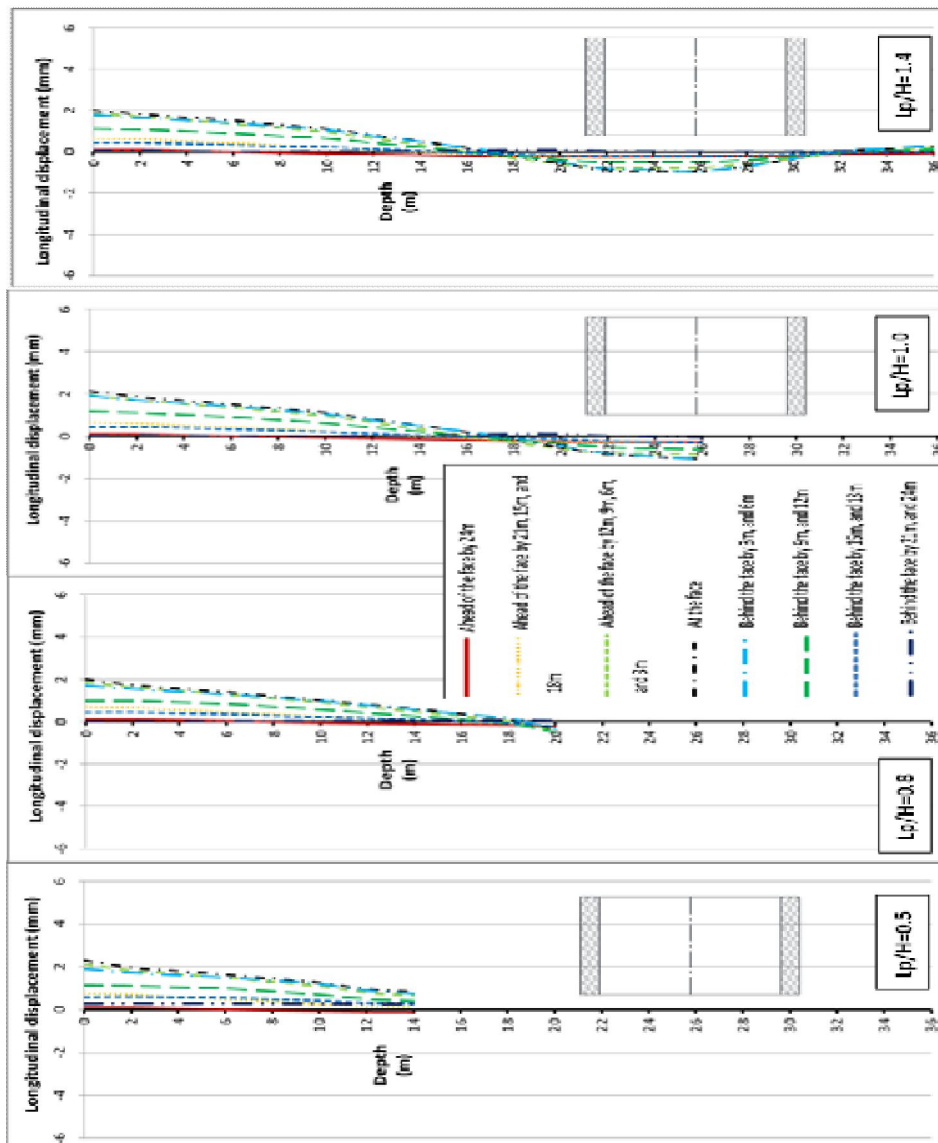


Fig.(6):  $L_p$  and constant offset from tunnel route ( $X_p=1.0D_t$ )

### 5.3. Lateral Displacement

The piles lateral displacement associated with tunnelling activities are indicated in Figs. (7 & 8). Mostly, the upper part of the piles deflects towards the tunnel, while the piles portions located near the tunnel opening deflected in the opposite direction, depending on the pile configuration relative to tunnel boundaries. The pile lateral displacement increases as the tunnel advancement increases. For piles having ratios of ( $L_p/H=0.5$ , and  $L_p/H=0.6$ ), the whole pile length deforms towards the tunnel with decreasing rate towards the tip and the lateral displacement of the pile tip is about half that at the pile head. This may be attributed to developed gap above tunnel crown where

the restraining effect took place (Yang et al., 2011). For a pile located as ( $L_p/H=0.8$ ,  $L_p/H=1.0$ , and  $L_p/H=1.4$ ), the tip deforms away from the tunnel opening with maximum deformation at the end of pile length except the case of  $L_p/H=1.4$  where, the maximum displacement occurs at the level of the springline and approximately reaches zero at the end of pile. This can be accredited to the soil-lining interaction phase and the lining ovaling mode of deformation. The lateral head deformation of pile with  $L_p/H=1.4$  is smaller than that of shorter pile by about 0.75. It may be noted that the maximum lateral displacement of the pile head occurs when the TBM is ahead of the pile cap by 9m-12m.

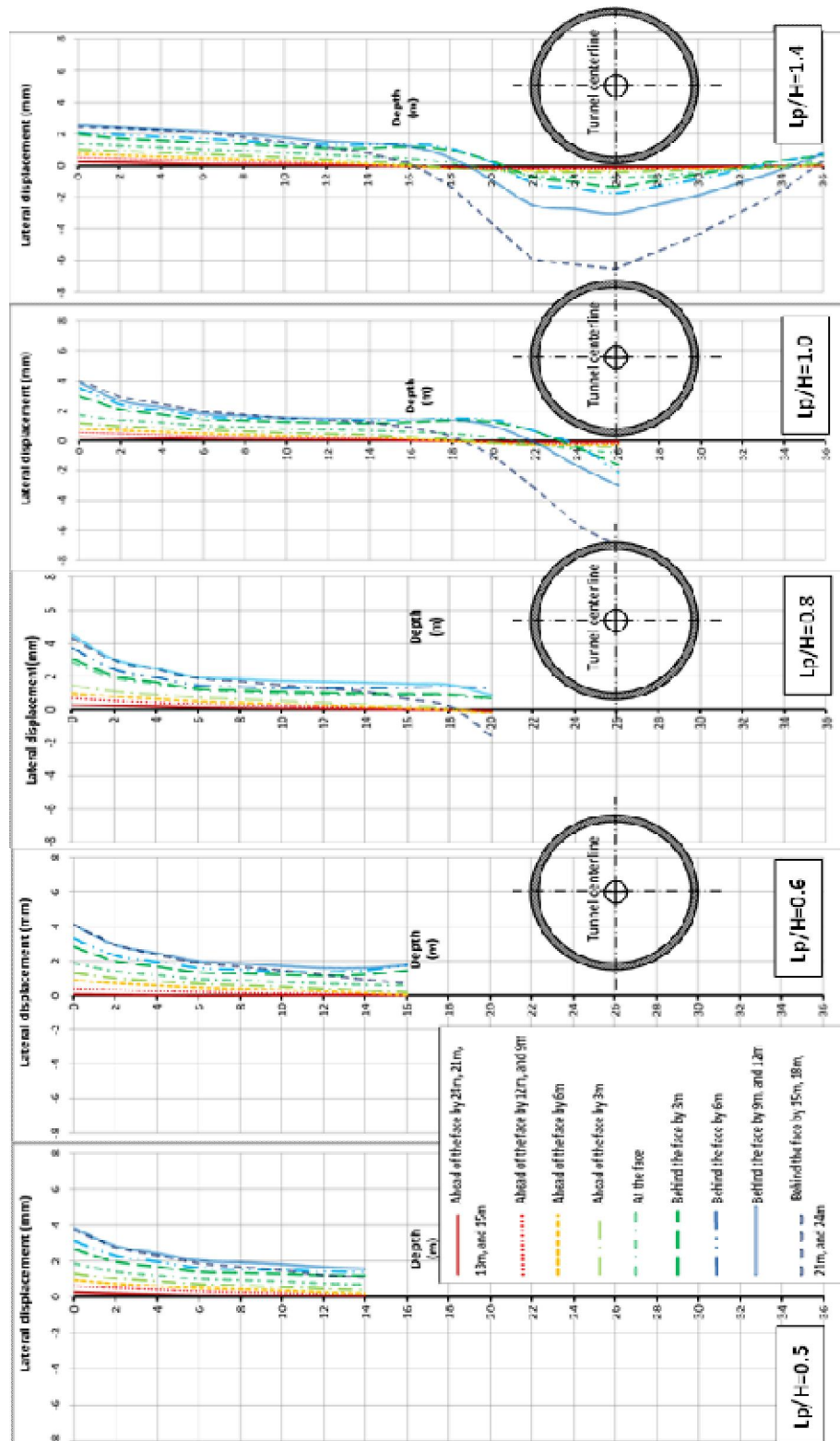


Fig.(7): Lateral displacement of front pile (1B) due to tunnelling for different values of ( $L_p/H$ ) and at constant offset ( $X_p=0.7D_t$ ).

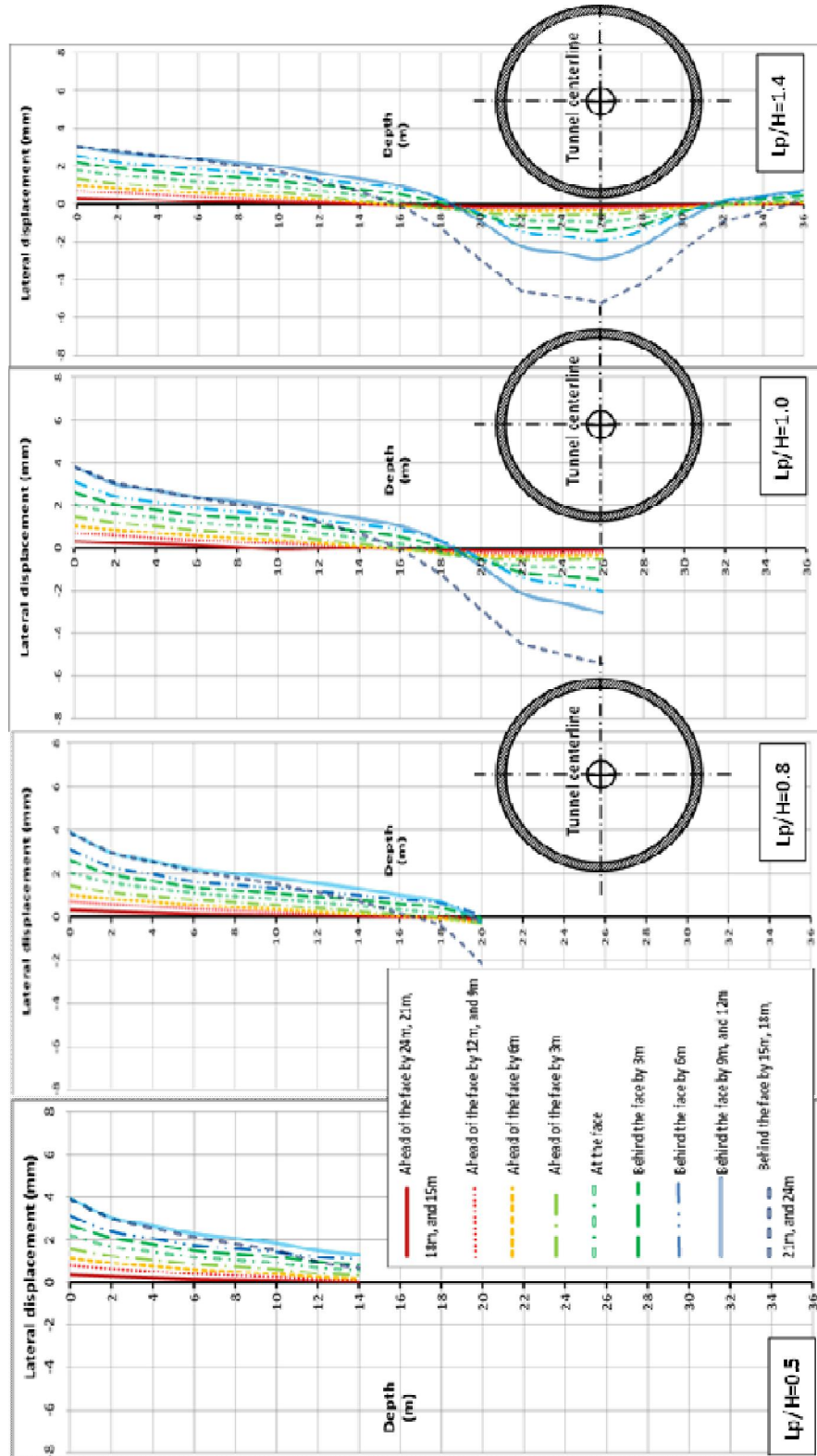


Fig.(8): Lateral displacement of front pile (1B) due to tunnelling for different values of  $(L_p/H)$  and at constant offset ( $X_p=1.0D_t$ ).



#### 5.4 Axial Force

Figure (9), demonstrates the distribution of the developed maximum axial piles forces due to tunnelling for the different ( $L_p/H$ ) ratios and offset distance ( $X_p/D_t$ ) ratio of 0.7 and 1.0. Both compressive and tensile forces are induced all-over the pile length due to tunnelling. The results indicate that the axial developed force increases as the ratio (pile length / tunnel depth) increases. For the case of ( $L_p/H < 1$ ), the pile is subjected to tensile force. A maximum tensile force of 126.3 kN is induced for pile ( $L_p/H=0.6$  and  $X_p/D_t=0.7$ ), which is less than the allowable tensile

capacity of pile (885 kPa). However, for the case of ( $L_p/H \geq 1$ ), negative skin friction is developed along the pile shaft and mobilize drag load, which increases with the depth and reaching its maximum value above the tip then decreases. The depth of maximum drag load varies between 0.7 to 0.8  $L_p$  depending to the length ratio ( $L_p/H$ ). The maximum axial compressive force achieved along the pile shaft in case of ( $L_p/H > 1$ ) is about 1253 kN which is larger than, the allowable compressive force (1200kN), according to the drawings of Mocarthy Brothers Company,(1984).

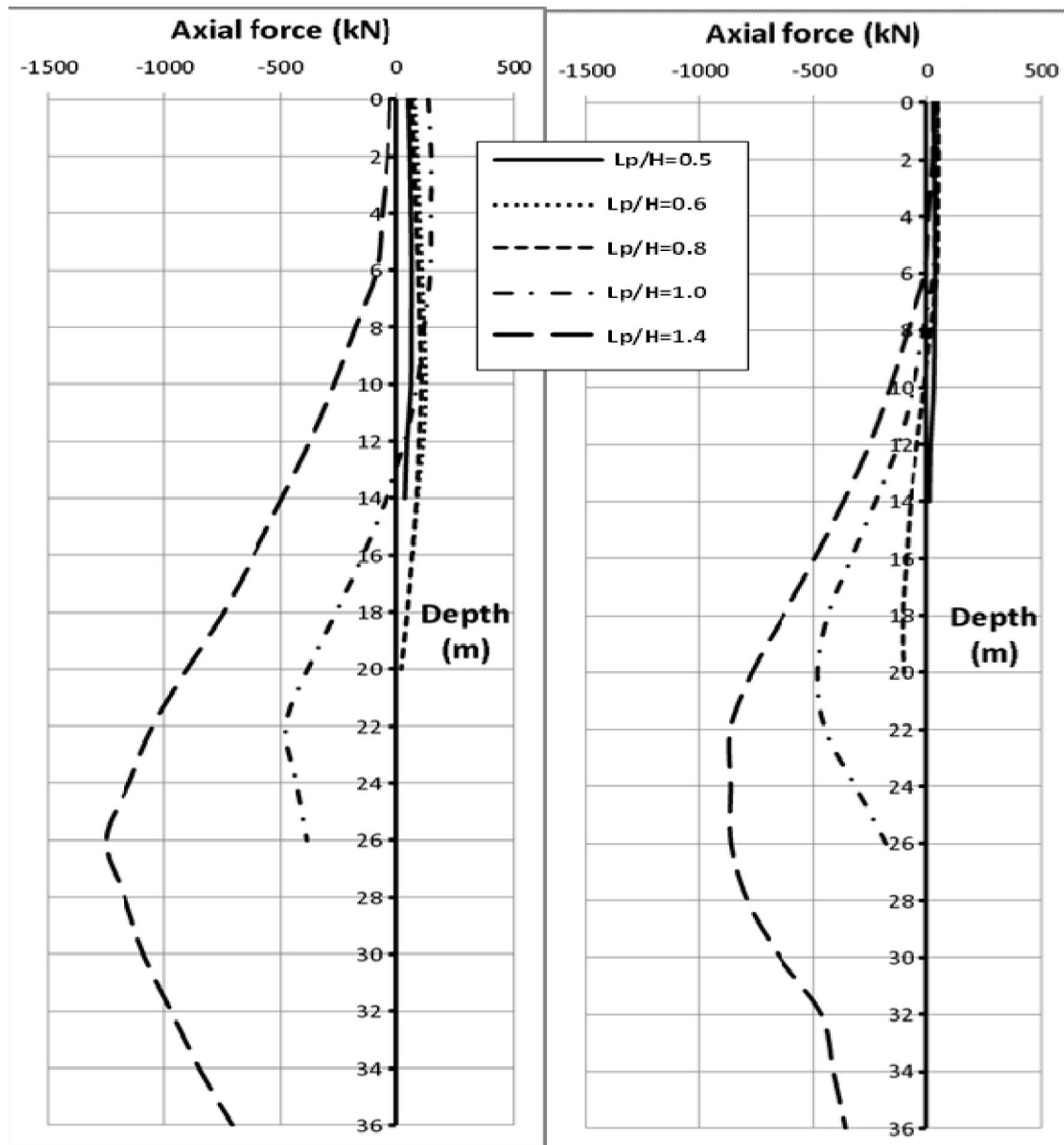


Fig.(9): The maximum axial force developed in the front pile (1B) for different pile lengths and for offset values  $X_p=0.7D_t$  and  $X_p=1D_t$

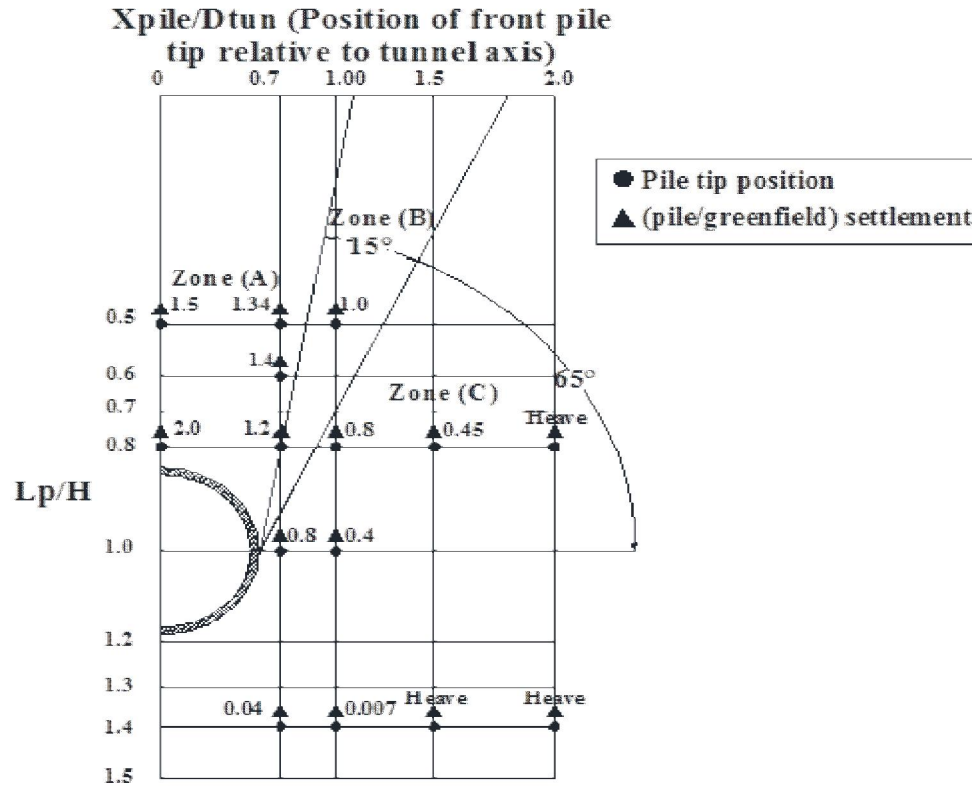


Fig.(10): Front pile/ Green-field surface settlement ratio.

## 6. Discussion

The results of the parametric study indicate that the configuration of the pile relative to the tunnel vicinity is considered as the main factor in the ground-tunnelling-pile analysis. Fig. (10), specifies the movement of the nearest pile relative to the green-field condition. It may be noticed that the pile tips located at or below the level of springline settle less than the green-field condition. Relatively, maximum settlement is detected for piles located directly above the crown  $L_p/H = 0.5, 0.6, 0.7,$  and  $0.8$  with maximum value for ( $L_p/H=0.8$ ). Simultaneously, as the offset distance of the cap increases, the pile cap relative settlement decreases. Accordingly, characterized zones (A, B, and C) can be identified by two proposed lines oriented from the tunnel spring line, as shown in figure (10). The first line deviates with an angle of  $(45^\circ + \phi/2)$  to the horizontal, while the second line diverges extra angle of  $(15^\circ)$ . The piles located in Zone (A) subjected to settlement values greater than the maximum order of the surface settlement profile depending on the tip distance to the tunnel crown. For piles positioned in Zone (B), it is expected that, the pile settlement is within the distribution of the settlement trough profile. For behaviour of piles localized in Zone (C) is completely independent of tunnelling influence. This proves that the maximum ground movements due to

tunnelling occurs near and/or at the crown zone and decreases outwards and downwards.

Figure (11), indicates the axial force ratio generated in the analysed piles. The axial force ratio is calculated as relating the induced forces due to tunnelling to the allowable forces per pile, (allowable compression = 1200kN, allowable tension=885kN). Accordingly, only the settlement criterion to check the safety of the deep foundation structures adjacent to the tunnel route is not enough, and it must be coupled by the analysis of developed forces due to tunneling to provide the characteristic zones (A, B, and C).

The induced stresses (axial force and bending moment) must be considered also as an important factor in the acceptance criterion. Although long pile located in Zone (C) exhibits settlement less than the green-field condition, but the induced compression force is very high (twice the permissible load), particularly for offset value less than  $X_p \leq D_t$ . Therefore, the induced forces in piles positioned within offsets  $X_p \leq D_t$  and length  $L_p \geq H$  is high and considered unsafe, (Zone CI). For piles located as  $D_t < X_p < 1.5D_t$ , the induced stresses is intermediate (less than 50% of the permissible), (Zone CII). For Piles with variable lengths placed with offset greater than  $1.5D_t$ , the generated axial loads are very small (less than 10% of permissible) (Zone CIII). Zone (B) characterized with

small settlement (equal to the green-field condition) and with small induced axial force (about 10%), can be specified as Zone CII). The piles situated in zone (A), suffers from great settlement values particularly those located above the crown, and the maximum induce

tension force along the pile shaft is less than the permissible load. Thus this zone is characterized by high settlement of the piles and intermediate induced stresses.

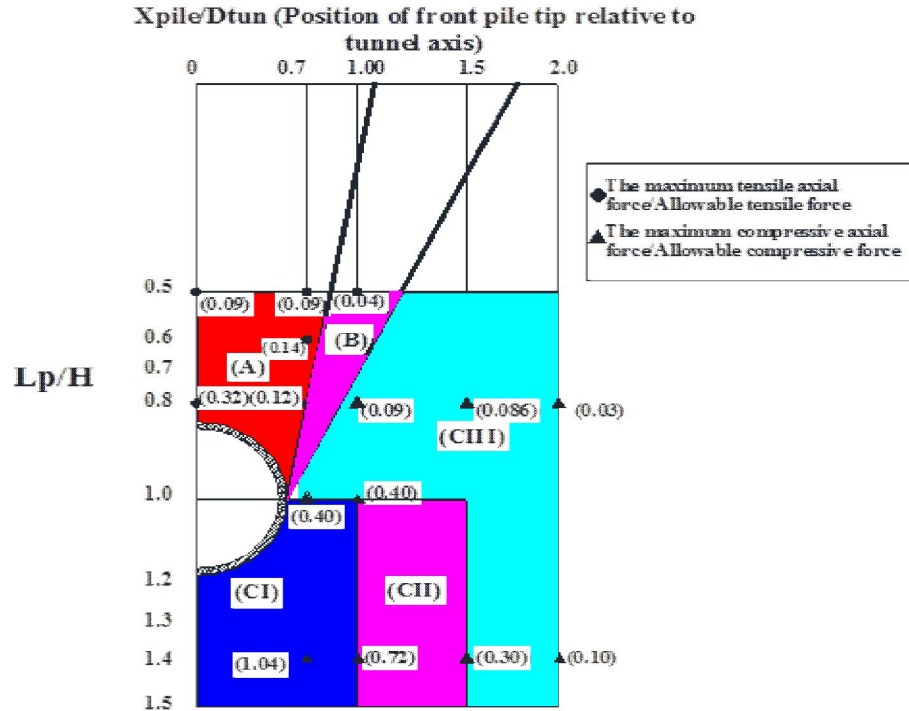


Fig.(11): Zone of distress.

### Conclusion

Based on the results of 3D finite element idealization concerning the ground-tunnelling-piled structure interaction; the following may be concluded;

- Tunnelling through soft ground conditions nearby buildings or utilities is a typical three dimensional idealism, particularly for piled foundations systems. The modelling of the ground-pile-tunnelling must take into the numerical consideration the details of tunnelling consequences, ground, lining, and grout behaviour and the nature of interaction through different phases. Also the details of the piles must be assigned in the interaction details.

- The results of pile settlement and pile induced forces due tunnelling for different (pile length/tunnel depth) and (pile eccentricity/tunnel diameter) ratios identified three specific zones around tunnel vicinity, definite as A, B, and C. The piles rested in the first zone is characterized by settlements greater than the green-field condition, while the second zone settlements is categorized inside the green-field condition, and the third is unaffected by tunnelling. These zones must be revised regarding to the piles induced straining forces associated with each zone.

Although long pile located in zone (C) exhibits settlement less than the green-field condition, but the induced compression force is very high and the zone may be specified as CI, CII, and CIII based on the developed stress criterion.

- For piles located in zone (B), the pile head moves laterally more than the pile tip towards the tunnel, while those positioned in zone (C), a smaller pile head deflection is observed. For piles placed at or below the springline, the maximum developed lateral displacement and bending moment occurs nearby the tunnel opening.

- The piles lateral deformations due to tunnelling are dictated in the transverse direction and insignificant in the longitudinal direction, acutely after the TBM passing the pile cap.

- For piles placed in zone (A) and/or zone (B), they are mainly subjected to tensile force, and those located in zone (C) are exposed to drag load all over the pile shaft due to the development of negative skin friction. Generally, the induced axial force increases as L<sub>p</sub>/H value increases and X value decreases.

**References**

1. Cheng, C.Y., Dasari, G.R., Leung C.F., Chow, Y.K. and Rosser, H.B. (2004). "3D Numerical Study of Tunnel-Soil-Pile Interaction", Proceedings of World Tunnel Congress and 13th ITA Assembly, Singapore.
2. Coutts, D. R. and Wang, J. (2000). "Monitoring of reinforced concrete piles under horizontal and vertical loads due to tunnelling". Tunnels and Underground Structures (eds. Zhao, Shirlaw & Krishnan), Balkema.
3. Dias, T.G.S., and Bezuijen, A. (2014). "Pile-tunnel interaction: A conceptual analysis" Geotechnical Aspects of Underground Construction in Soft Ground – Yoo, Park, Kim & Ban (Eds), Seoul, Korea, ISBN 978-1-138-027008.
4. Hibbitt, Karlsson & Sorensen, Inc (2011). ABAQUS User's manual, Version 6.11.
5. Lee, C.G. (2012). "Three-dimensional analyses of the response of a single pile and pile groups to tunnelling in weak weathered rock." Tunnelling and Underground Space Technology, Vol. 32, pp.132-142, DOI: 10.1016/j.tust.2012.06.005.
6. Lee, C., J. (2013). "Numerical analysis of pile response to open face tunnelling in stiff clay." Computers and Geotechnics, Vol. 51, pp.132-142, DOI:10.1016/j.tust.2012.06.005.
7. Lee, R.G, Turner, A.J., and Whitworth, L.J. (1994). "Deformations caused by tunnelling beneath a piled structure." Proc. The XIII International Conference on Soil Mechanics and Foundation Engineering, University Press, London, pp. 873-878.
8. Linlong, M., Maosong, H., and Richard, J.F. (2012). "Tunnelling effects on lateral behaviour of pile rafts in layered soil." Tunnelling and Underground space Technology, Vol.28, pp.192-201, DOI:10.1016/j.tust.2011.10.010.
9. Mocarthy Brothers company, (1984). A division of design and management, consultant of Ataba Parking Garage, Cairo, Egypt.
10. Morton, J.D. and King, K.H. (1979). "Effects of tunnelling on the bearing capacity and settlement of piled foundations". In: Proceedings of the Symposium Tunnelling'79. London.
11. Ng, C. W. W., Lu, H., and Peng, S. Y. (2013). "Three-dimensional centrifuge modelling of the effects of twin tunnelling on an existing pile." Tunnelling and Underground Space Technology, Vol.35, pp.189-199, DOI:10.1016/j.tust.2012.07008.
12. Pang, C.H., Yong, K.Y., and Chow, Y.K. (2005). "Three-dimensional numerical simulation of tunnel advancement on adjacent pile foundation", Analysis of the Past and Lessons for the Future – Erdem & Solak (eds), National University of Singapore, Singapore, ISBN 04 1537 452 9.
13. YANG Min, SUN Qing, LI Wei-chao, and MA Kang, (2011). "Three-dimensional finite element analysis on effects of tunnel construction on nearby pile foundation", J. Cent. South Univ. Technol, Vol.(18), pp.909-916.
14. Yao, A., Yang, X., and Dong, L. (2012). "Numerical analysis of the influence of isolation piles in metro tunnel construction of adjacent buildings." Procedia Earth and Planetary Science, Vol. 5, pp.150-154, DOI:10.1016/j.proeps.2012.01.026.
15. Zidan, A.F and Ramadan, O.M.O (2015). "Three dimensional numerical analysis of the effects of tunnelling near piled structures" J. of Korean society of civil engineering, Vol.(19), pp.917-928.

6/20/2015